

# Electronic and gap properties of lead-free perfect and mixed hybrid halide perovskites: An *ab-initio* study

Athanasios Koliogiorgos, Sotirios Baskoutas and Iosif Galanakis

*Department of Materials Science, School of Natural Sciences, University of Patras, GR-26504 Patra, Greece*

---

## Abstract

Hybrid halide perovskites are currently under intense investigation due to their potential applications in optoelectronics and solar cells. Among them, MAPbI<sub>3</sub> where MA stands for the methylammonium cation, exhibits ideal properties for solar cells. In attempt to identify new lead-free halide perovskites we have studied using *ab-initio* electronic structure calculations in conjunction with hybrid functionals a series of MABX<sub>3</sub> compounds where B is a divalent cation and X is a halogen atom. Our results suggest that the compounds under study exhibit a variety of lattice constants and energy band gaps. Especially, MAgCl<sub>3</sub> and MAgBr<sub>3</sub> are susceptible to replace MAPbI<sub>3</sub> in devices since they show comparable energy gaps. Further calculations on the mixed hybrid halide perovskites show that we can tune the values of the energy gap although no simplified pattern exists. Our results pave the way for further investigation on the use of these materials in technology relevant applications.

*Key words:* Halide perovskites, Density-functional theory, Electronic Band structure

*PACS:* 71.20.-b, 71.20.Nr, 71.15.Mb

---

## 1. Introduction

Renewable energy sources are essentially a one-way road for energy consumption in the 21st century, since the finite and limited supply of fossil fuels is bound to come to an end. The sun is a practically infinite energy source, and photovoltaic(PV) devices that turn the energy of sunlight into electricity are expected to become more prominent as a main renewable energy source [1]. Silicon is the most widely used material in solar cell technology, with a history of over 60 years [2]. Other types of solar cells used in PV technology include type III-V semiconductors, quantum dots, dye-sensitized solar cells, organic solar cells and perovskites.

Designated as perovskite is a material that has the general structure of ABX<sub>3</sub>. The most known perovskites are the ones where X is an oxygen. To achieve charge neutrality in that case, A has to be

a cation of +2 valence and B a cation of +4 valence of dissimilar size like in CaTiO<sub>3</sub> [3]. The versatility of perovskites makes them highly attractive as they can form multidimensional structures pertaining to the same chemical formula through use of different combinations of various components [4,5]. A wide variety of elements may be incorporated in the ABX<sub>3</sub> structure, as long as the requirement for charge neutrality is satisfied. Although oxide perovskites are the most well-studied and widely used in applications due to their multifunctional nature, their wide band gaps limit their use in solar cell technology, as they utilize a mere 8-20% of the solar spectrum [3].

To overcome the poor absorption of the oxygen perovskites, other types have been proposed like the halide perovskites where the X anion is a halogen instead of oxygen and mainly the so-called hybrid or organometallic halide perovskites,

where the A cation is an organic molecule [1,5–7], offering the ability to tune the photoconductive properties through varying halide components [8]. Their success is based on a highly favorable charge-carrier mobility so that both light absorption and charge conduction are possible [9]. One of the most widely used organic cations is methylammonium (MA) which has the chemical formula  $\text{CH}_3\text{NH}_3^+$  [1]. Especially the one containing lead as the divalent cation and iodine as the halogen,  $\text{MAPbI}_3$ , has attracted most of the attention [10–12], and its growth conditions have been widely studied [13,14].

$\text{MAPbI}_3$  has an experimental gap of 1.5 eV, which makes it suitable for absorption in the optical regime [15]. More recent experimental results on cubic crystals of  $\text{MAPbI}_3$  gave a value of 1.69 eV at 330 K [16]. Although several of its properties and their effect on the band gap have been widely studied, such as the influence of the orientation of the MA atoms [17–19], the toxicity of the lead atoms led to the search for alternative hybrid halide perovskites [20]. *Ab-initio* electronic structure calculations have been also employed in this search. Sn, which is isovalent to Pb, has been proposed as a replacement but it oxidizes very easily and the perovskite structure is destroyed [21,22]. Sr replacement for Pb in  $\text{MAPbI}_3$  leads to an energy gap double the initial one and thus cannot be applied in PV applications [23]. The partial substitution of I atoms with other halogen influences the energy width of the band gap but does not solve the toxicity problem [24,25].

Motivated by the search for lead-free hybrid halide perovskites, we carry out an extended *ab-initio* study of the  $\text{MABX}_3$  compounds. As X we have considered all possible halogen atoms, namely F, Cl, Br and I. Divalent B cations can be either the alkali earth elements (Ca, Sr, Ba) since they have two valence  $p$  electrons, the late transition metal atoms (Zn, Cd, Hg) which have two valence  $s$  electrons and the metalloids (Ge, Sn, Pb) which have also two valence  $p$  electrons but contrary to the alkali earth elements the valence  $d$  states are completely occupied. For all 36 resulting compounds we have relaxed the position of the atoms and the C-N bond length of the MA cation and determined the equilibrium lattice constants. For the equilibrium lattice constants, we have employed advanced functionals of the exchange and correlation energies and have determined the width of the energy band gaps. Finally, we have also studied the possibility to tune the energy band gaps in mixed hybrid halide perovskites by mixing two kinds of halogen atoms

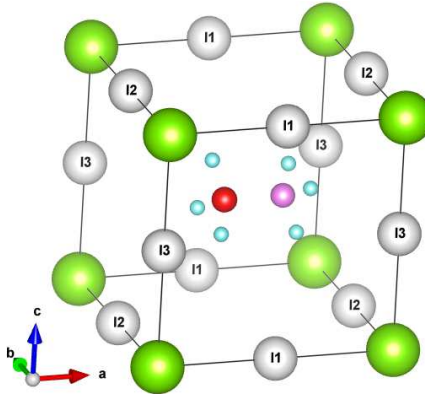


Fig. 1. Cubic unit cell of the  $\text{MABl}_3$  compounds. The divalent cations B (green spheres) are at the corners of the cube surrounded by six halogen atoms (grey atoms). There are three inequivalent halogen atoms in the unit cell at the midpoints of the edges. The C-N bond of the MA cation ( $\text{CH}_3\text{NH}_3$ ) is along the x-axis, and each one of the C (red sphere) and N (purple sphere) atoms is surrounded by three H atoms (light blue spheres). We also denote the Cartesian axis  $x$ ,  $y$  and  $z$  using the unit vectors  $\vec{a}$ ,  $\vec{b}$  and  $\vec{c}$ , respectively.

in the unit cell. In section 2 we present the details of our calculations. Section 3 is devoted to the structural properties of the compounds under study and section 4 to their electronic and gap properties. In section 5 we present our results on the mixed compounds and finally in section 6 we summarize and present our conclusions.

## 2. Computational method

We have calculated the structural and electronic properties of the hybrid halide perovskites under study employing the *ab-initio* total energy and molecular-dynamics program VASP (Vienna *Ab-initio* Simulation Package) developed at the Institut für Metalphysik of the Universität Wien [26]. We made use of the projector augmented waves (PAW), which are a generalization of the ultra-soft pseudopotentials used in conventional pseudopotential electronic structure methods [27]. To account for the exchange-correlation potential we have used the generalized gradient approximation (GGA) as formulated by Perdew, Burke and Ernzerhof (PBE) [28]. More precisely, we have employed the parametrization of PBE developed by Perdew et al. in reference [29] which restores the correct density-gradient expansion for the exchange energy in solids with respect to the initial PBE formalism

(known in literature as PBEsol).

Although GGA in general is known to reproduce accurately the structural properties, it presents a serious drawback regarding semiconductor materials: while the calculated band structure is qualitatively correct, the energy gap is largely underestimated. But the exact value of the energy gap is crucial for applications since it determines the wavelength of the absorbed light. To restore the correct value of the energy gap several methods have been proposed. One of the most rigorous is the use of more complex functionals where the exchange energy is a mixture of the GGA and Hartree-Fock functionals. These functionals are known as “hybrid functionals” and the most well-known in materials science is the Heyd-Scuseria-Ernzerhof (HSE06) functional [30], which has been successfully implemented in VASP [31]. Except HSE06, we have also performed calculations using the modified Becke-Johnson functional in conjunction with the PBEsol one (known as mBJ+PBEsol). The mBJ has been developed in 2006 by Becke and Johnson in an attempt to provide an efficient exchange functional which would reach the accuracy of the hybrid functionals like HSE06 but which would need similar CPU resources like GGA [32] contrary to HSE06 based calculations which are very demanding. It became popular in 2009 when Tran and Blaha introduced it in the full-potential (linearized) augmented plane wave and local orbitals [FP-(L)APW+lo] method and found that it gives band gaps for a series of insulators and semiconductors close to the HSE functionals [33]. We should also note that the mBJ functional, actually, is a potential-only functional being a local approximation to an atomic exact-exchange potential plus a screening term which is used in conjunction to one of the exchange-correlation schemes (PBEsol in our case). Thus the mBJ-based calculations within VASP are not self-consistent with respect to the total energy contrary to the HSE06 or PBEsol functionals (details are given in the online manual of VASP [34]).

We should also shortly discuss the accuracy of the various functionals to study the compounds of interest. Although calculations using HSE06 are expected to give more accurate results than the usual GGA functionals and mBJ calculations are expected to reach the accuracy of HSE06, in reality the success of the HSE06 and mBJ functionals is materials specific and it is established only when the computed values are compared to the experimental ones. HSE06 has been applied with success to the study of

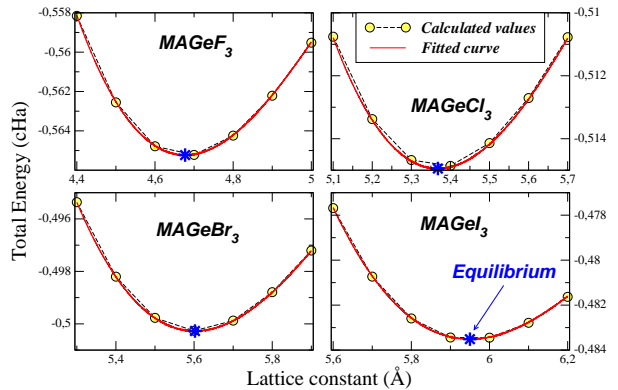


Fig. 2. Calculated total energy versus the lattice constant in MAGEX<sub>3</sub> compounds. The calculated values have been fitted with a third order polynomial in order to determine the equilibrium lattice constant. Note that the use of the Murnaghan equation of state gives identical results in the case of the compounds under study.

the electronic properties of the oxygen perovskites [35]. Moreover, recent experiments on cubic crystals of MAPbI<sub>3</sub> by Quarti and collaborators produced a value of 1.69 eV at 330 K [16]. As will be discussed in section IV, PBEsol produces a value of 1.49 eV, while HSE06 and mBJ+PBEsol produce values of 1.82 eV and 1.85 eV, respectively. Since ab-initio calculations are carried out at 0 K and the width of the band gap drops with the temperature, we expect that our calculated HSE06 and mBJ+PBEsol band gap values are close to the experimental one. All the above provide strong evidence that HSE06 and mBJ+PBEsol are suitable to study the halide perovskites, although more experimental results on crystals are needed for definitive conclusions.

Concerning the details of the calculations, we have used for all of them a cutoff for the kinetic energy of the plane waves of 500 eV and for the Ge, Sn and Pb atoms we have included in the PAW basis the 3*d*, 4*d* and 5*d* orbitals, respectively, as valence states. For the case of the mBJ+PBEsol calculations we have used a more advanced basis set including also the kinetic energy density of the core electrons. In order to establish the accuracy of our calculations we have calculated MAPbI<sub>3</sub> as a test case, since it is the most studied compound in literature. The obtained results were in perfect agreement with the existing ones in literature [17], as will be discussed later.

### 3. Structural properties

The hybrid halide perovskites under study crystallize in a cubic structure shown in figure 1 [19]. The divalent cations sit at the corners of the cube surrounded by halogen atoms in an octahedral environment. The MA cation sits at the center of the cube. The first step in our study is the determination of the equilibrium lattice constant. To determine it for all the compounds we have performed total energy calculations for several lattice constants using a  $6 \times 6 \times 6$  Monkhorst-Pack grid in the 1st Brillouin zone [36] in conjunction with the PBEsol functional. For each lattice constant we fixed the position of the divalent cation and the halogen atoms. We allowed the MA atom to fully relax within the cell (the positions of all C, N and H atoms have been allowed to change). The only constraint, which was imposed, was that the C-N bond stays parallel to the [100] direction passing from the center of the cube. In reality as shown in reference [19] the MA cations can rotate in very short times but such a picture cannot be captured by conventional electronic structure calculations. Moreover, test calculations for MAPbI<sub>3</sub> have shown that the orientation of the MA cation is not decisive for the obtained values of the band gap. We have chosen 7 values around the equilibrium and fitted a third order polynomial curve to determine the equilibrium lattice constant corresponding to the minimum of the energy. In figure 2 we show the calculated total energy values versus the lattice constants as well as the fitted curve for the four MAGEX<sub>3</sub> compounds. Although the curve has different curvature for each of these compounds, the fitting is excellent and the fitted curve passes in all cases through all seven calculated points.

We have gathered the calculated equilibrium lattice constants in Å for all 36 calculated compounds and present them in table 1. The obtained equilibrium lattice constants scan a wide range of values starting from 4.4958 Å in the case of MAZnF<sub>3</sub> up to 6.7362 Å for MABaI<sub>3</sub>. As expected, the trends follow the size of the atomic radius of the constituent atoms. As we move from the light F halogen to the heavy I atom, keeping the divalent cation B constant, the equilibrium lattice constant increases in all cases by about 30%. Differences are much smaller if we fix the halogen atom and change the B cation within the same row. We can compare our calculated values with previous calculations and experiments in the case of MAPbI<sub>3</sub> for which data exist

Table 1

Calculated equilibrium lattice constants,  $a_{eq}$ , in Å for the hybrid halide perovskites using the PBEsol approximation. These perovskites have the chemical formula MABX<sub>3</sub> where MA is the methylammonium cation (CH<sub>3</sub>NH<sub>3</sub>), B is a divalent cation and X is a halogen atom.

$a_{eq}^{\text{MABX}_3}$ (Å)	X=F	X=Cl	X=Br	X=I
B=Ca	4.7059	5.4883	5.7590	6.1709
B=Sr	4.8907	5.7103	5.9886	6.4127
B=Ba	5.1694	6.0142	6.3127	6.7362
B=Zn	4.4958	5.1723	5.4276	5.8133
B=Cd	4.6656	5.3548	5.6088	5.9923
B=Hg	4.7385	5.4047	5.6563	6.0203
B=Ge	4.6771	5.3679	5.6023	5.9499
B=Sn	4.8581	5.6047	5.8431	6.2021
B=Pb	4.9354	5.7006	5.9454	6.3134

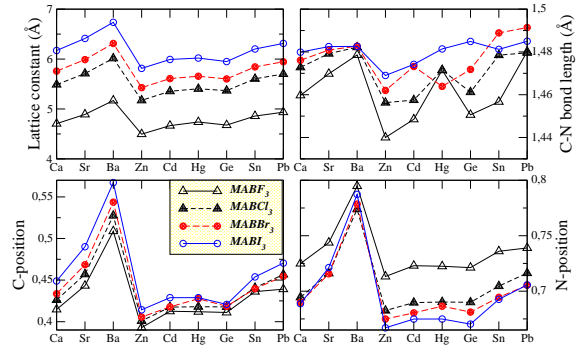


Fig. 3. Behavior of the equilibrium lattice constant (upper left panel), C-N bond length (upper right panel) in Å, and the position of the C and N atoms of the MA cation (lower panels) in units of the lattice constant as a function of the divalent cation.

in literature. Powder diffraction experiments gave a value of 6.26 Å [37], while calculations give values between 6.26 Å and 6.33 Å [17,24], which are very close to our calculated value of about 6.31 Å.

It is interesting also to study the behavior of the MA cation in the studied compounds. In figure 3 we have gathered all the related results as a function of the divalent B cation. The four curves in each panel correspond to the four halogen atoms under study. In the upper left panel, we first present the behavior of the equilibrium lattice constants. All four curves are parallel and thus for each divalent cation B, the halogen atoms affect the lattice constant in the same manner. In the upper right panel we present the behavior of the C-N bond length. The latter in general follows the behavior of the equilib-

rium lattice constants but there are exceptions, *e.g.* the length is larger for MAPbBr<sub>3</sub> than MAPbI<sub>3</sub>. The bond length does not show large variations being the smallest for MAZnF<sub>3</sub> (about 1.44 Å) and the largest for MAPbB<sub>3</sub> (about 1.49 Å), a variation of about 3.5% only. In the lower panels in figure 3 we present the position of the C and N atoms as a fraction of the lattice constant. First, we have to note that in all cases the MA cation is not centered around the middle of the cube resulting in the appearance of a dipole where the N atom is more distant from the cube’s center. The Ba-based compounds are an exceptional case since the MA cation is completely off-center and both C and N atoms are on the right side of the cube’s center. Thus, it is possible to find ferroelectric behavior in these compounds. Finally, we should note that, although all curves for the different structural properties in figure 3 follow the shape of the lattice constant curves in the upper left panel, we were not able to deduce some strict rules as is the case in other phenomena [38].

#### 4. Electronic and gap properties

Since we have determined the equilibrium lattice constants, we proceeded with the calculation of the energy gaps which is also the main finding of the present study. We have used a much denser 10×10×10 Monkhorst-Pack grid to carry out the self-consistent electronic band structure calculation at the equilibrium lattice constants. First, we employed the PBEsol functional. As mentioned above, the former is not accurate enough in most cases to compute the energy gaps, and thus we used the PBEsol calculated electronic charge and wavefunctions as the input to perform electronic band structure calculations with the most accurate and much more demanding in computer resources hybrid HSE06 functional as well as the more efficient mBJ+PBEsol using the same grid in the reciprocal space as for the PBEsol calculations. In table 2 we have gathered the HSE06 calculated energy gaps for all 36 six compounds under study as well as the mBJ+PBEsol and PBEsol results in braces and parentheses, respectively. In all cases under study, the use of HSE06 and mBJ+PBEsol leads to larger values for the band gaps with respect to the PBEsol functional. All three functionals give the same trends within the table as we change either the divalent B cations or the X halogen atom, but the effect of HSE06 with respect to PBEsol

is not uniform in all cases. *E.g.* for MAZnF<sub>3</sub> the HSE06 gap is almost two times the PBEsol gap while in MACaF<sub>3</sub> the increase is only 25%. Also the behavior of mBJ+PBEsol is not uniform in all cases. In almost all cases mBJ+PBEsol gives band gaps smaller than the HSE ones, but there are compounds like MACaCl<sub>3</sub> where the mBJ+PBEsol is closer to the PBEsol than the HSE06 value, and there are compounds like MAGeI<sub>3</sub> and MAPbI<sub>3</sub> where both HSE06 and mBJ+PBEsol produce identical values. Interestingly, in the case of the gapless-semiconducting compounds like MAZnI<sub>3</sub> all three functionals give identical results. Thus, the effect of the HSE06 and mBJ+PBEsol functionals on the calculated energy gap values is materials specific.

For all cases of the divalent B cations, the energy band gap becomes considerably smaller as we change the halogen atom going from the light F to the heavy I one, with the largest variation being observed in the cases of the Zn, Cd and Hg cations. This is expected since the lighter the halogen atom is, the deeper are its valence *p* states and the larger is the energy gap, *i.e.*, in the case of F the valence states are the 2*p* orbitals while in the case of I the valence states are the 5*p* orbitals which are much higher in energy (see figure 4). Our calculated values are in agreement with previous calculations where available. More precisely the energy gap for MASrI<sub>3</sub> using PBEsol was estimated to be 3.6 eV [23], very close to our value of 3.52 eV. For MAPbI<sub>3</sub>, values of 1.5 eV using PBEsol and about 2.0 eV using the HSE06 functional have been obtained [17]. Our PBEsol value, as shown in table 2, is 1.49 eV, identical to the one in literature, while our HSE06 value is 1.82 eV -slightly smaller than the 2 eV in literature.

We can categorize the materials presented in table 2 in three categories depending on the B cation. When B is an alkali earth atom (Ca, Sr or Ba) the calculated energy gaps are very large exceeding the 4 eV, with the exception of MABaI<sub>3</sub> where it is about 3.9 eV using both HSE06 and mBJ+PBEsol. For the case of X=F they are even close to 7 eV. These values are very large and by far exceed the values of 1.5-1.8 eV required in order to absorb in the optical regime. As a consequence, these materials are transparent to the visible light. When the cation is Zn, Cd or Hg energy gaps are considerably smaller. There is the case of MAZnCl<sub>3</sub> and MACdBr<sub>3</sub> where the gap is 1.94/1.80 eV and 1.30/1.21 eV, respectively, using the HSE06/mBJ+PBEsol functionals, and thus could be useful for applications, although Cd is a toxic material like Pb. But it is also widely

Table 2

Calculated energy gap in eV using the HSE06, the mBJ+PBEsol [in braces], and PBEsol functionals (the latter in parentheses) for the  $\text{MABX}_3$  hybrid halide perovskites. The zero values correspond to a gapless (zero-gap) semiconducting behavior.

$\text{MABX}_3$	Band gap (eV)			
	X=F	HSE06 [mBJ+PBEsol] (PBEsol)		
		X=Cl	X=Br	X=I
B=Ca	7.71[7.30](6.20)	6.30[5.20](4.80)	5.36[4.63](4.30)	4.00[3.57](3.40)
B=Sr	7.57[7.28](5.92)	6.30[5.70](4.92)	5.26[5.08](4.15)	4.23[4.00](3.52)
B=Ba	6.91[6.53](5.33)	5.84[5.30](4.89)	5.02[4.64](4.26)	3.86[3.84](3.27)
B=Zn	3.78[3.35](1.96)	1.94[1.80](0.81)	0.71[0.84](0.12)	0.00[0.00](0.00)
B=Cd	4.47[4.05](2.90)	2.42[2.11](1.52)	1.30[1.21](0.57)	0.22[0.23](0.00)
B=Hg	1.84[1.62](0.70)	0.23[0.00](0.00)	0.00[0.00](0.00)	0.00[0.00](0.00)
B=Ge	4.12[3.33](2.66)	1.96[1.64](1.33)	1.51[1.37](1.07)	1.21[1.22](0.93)
B=Sn	3.61[3.07](2.24)	1.70[1.55](1.07)	1.19[1.10](0.84)	0.94[0.86](0.72)

[1.85](1.49)

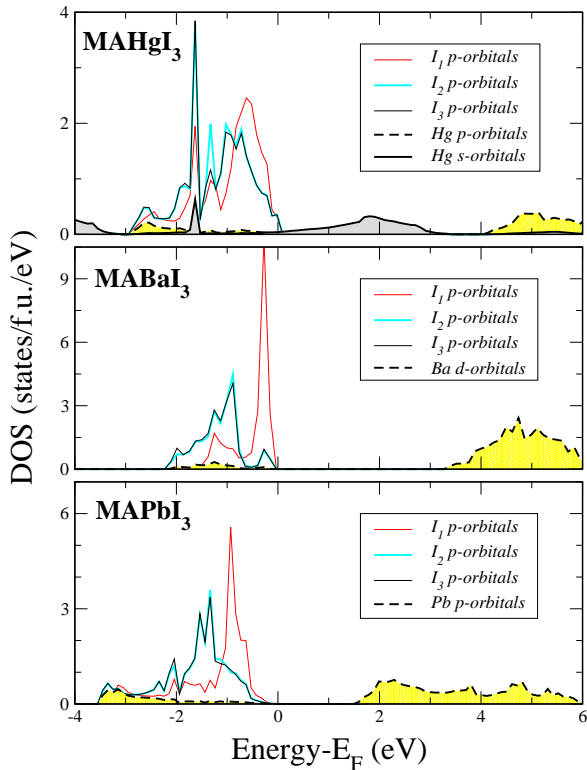


Fig. 4. Orbital and atom-resolved density of states (DOS) as a function of the energy for  $\text{MA}(\text{Hg}, \text{Ba}, \text{Pb})\text{I}_3$  compounds using the PBEsol functional. The zero energy corresponds to the Fermi level. The valence bands consist of the I  $p$ -orbitals. The conduction bands are made up from the Ba, Hg or Pb states. The kind of hybridization determines the width of the energy gap. Note that the use of HSE06 or mBJ+PBEsol functional opens the gap but does not influences the character of the bands.

used in compounds like, *e.g.*, the CdSe quantum dots for LED applications. Some very interesting cases are all three compounds with I, as well as  $\text{MAHgBr}_3$  where the energy gap is very small or zero. Such nearly-gapless or gapless semiconductors are interesting for spintronic applications due to the high mobility of carriers and the very small amount of energy needed to excite the electrons. Finally, we have the case where the cation is one of the metalloids Ge, Sn or Pb. Sn halide perovskites have been suggested in literature as a possible substitute for the Pb ones, but they are unstable and the Sn atoms are oxidized very easily going from a +2 to a +4 state, destroying the perovskite structure [22]. Thus the case of the Ge perovskites becomes much more interesting. The Ge based halide perovskites show band gaps slightly smaller than the Pb-based ones. Both  $\text{MAGeCl}_3$  and  $\text{MAGeBr}_3$  with band gaps of 1.96 eV and 1.51 eV within HSE06 (mBJ+PBEsol gives slightly smaller values), respectively, are susceptible of absorbing light in the visible region and thus could be employed in solar cell applications instead of  $\text{MAPbI}_3$  used in current solar cells.

To elucidate the trends observed in the calculated band gap energies, we have plotted in figure 4 the atom- and orbital resolved density of states (DOS) for three compounds  $\text{MA}(\text{Hg}, \text{Ba}, \text{Pb})\text{I}_3$  using the PBEsol functional; HSE06 and mBJ+PBEsol functionals affect the width of the band gap but not the character of the bands. In all three cases the valence bands are made up from the  $p$  states of the iodine atoms. There is also a very small  $s$  admixture which is not shown here. Note that there are

three inequivalent I atoms denoted as  $I_1$ ,  $I_2$  and  $I_3$  (for the definition please refer to figure 1).  $I_2$  and  $I_3$  are almost equivalent with respect to the position of the MA cation and thus have very similar DOS which cannot be distinguished. On the contrary,  $I_1$  is located in the middle of the [100] edge and has a distinctively different DOS with its  $p$ -states occupying the higher part of the valence bands. In the case of  $\text{MAPbI}_3$  the conduction band is made up from the Pb empty  $6p$  states and thus the gap is due to the  $p$ - $p$  hybridization, in agreement with previous *ab-initio* results [12]. Similar is the situation when instead of Pb we have the isovalent Sn or Ge cations. In the case of alkali earth cations the conduction band is now made up from the unoccupied  $d$  orbitals (the unoccupied  $p$  states are higher in energy) and more precisely the triple degenerate  $t_{2g}$  orbitals which transform in the same way as the  $p$  orbitals in the case of tetrahedral and octahedral symmetries, *i.e.* in the case of  $\text{MABaI}_3$  shown in figure 4 the conduction band consists of the Ba  $5d$  orbitals and the  $6p$  orbitals are higher in energy. Therefore the main interaction responsible for opening the gap is the  $p$ - $d$  hybridization which is not as strong as the  $p$ - $p$  one and the gap is larger. Finally, when the cation is Zn, Cd or Hg, a conduction  $s$ -state appears clearly between the occupied  $p$  states of the halogen atoms and the unoccupied  $p$  states of the Zn, Cd or Hg atoms. Thus although the  $p$ - $p$  hybridization opens a sizeable gap, the location of the Zn, Cd, or Hg  $s$ -states within the gap leads to much smaller energy gap values and even to the observed gapless behavior as in the case of the  $\text{MAHgI}_3$  compounds shown in the upper panel of figure 4.

## 5. Mixed halide perovskites

In the last part of our study we have concentrated on the so-called mixed hybrid halide perovskites [24]. The idea is to seek whether by mixing the halogen atoms, one could result in tuning the energy gap. We have employed the PBEsol formalism since, as discussed in the previous section, PBEsol accurately reproduces the correct trend with respect to the other two more elaborated functionals. We have assumed for all the studied compounds that the lattice constant varies linearly between the equilibrium lattice constants. Thus for the  $\text{MAB}(X_2X')$  compound the lattice constant is

$$a_{\text{MAB}(X_2X')} = \frac{2}{3}a_{\text{MABX}_3} + \frac{1}{3}a_{\text{MABX}'_3}. \quad (1)$$

To validate our assumption, we have also computed the equilibrium lattice constant using total energy calculations as for the perfect compounds in the case of the Pb-mixed halide perovskites; the calculated values differ less than  $0.02 \text{ \AA}$  from the values deduced using equation 1. Thus the deviation is less than 0.3 %, which has negligible effect on the calculated electronic properties, and we can safely use equation 1.

For all studied mixed compounds, the MA cation was relaxed similarly to the ordered compounds described above. In the case of the  $\text{MAB}(X_2X')$  there are three different configurations depending on the position of the  $X'$  atom. We denote them as cases I, II and III depending on whether the  $X'$  atoms substitute the  $X_1$ ,  $X_2$  or  $X_3$  atom, respectively (this notation follows the nomenclature introduced in figure 1 for the I atoms). Also, for each lattice constant we have recalculated the energy gap for both  $\text{MABX}_3$  and  $\text{MABX}'_3$  parent compounds since the value of the energy gap is lattice constant dependent and differs from the value at the equilibrium lattice constant calculated and presented in the previous section.

We have gathered the calculated energy band gaps for the mixed hybrid halide perovskites in table 3. First, we have to remark that the energy gap for the same compound can differ substantially with the lattice constant. *E.g.*  $\text{MAPbI}_3$  has a gap of 1.01 eV at the lattice constant of  $\text{MAPb}(\text{Cl}_2\text{I})$ , 1.30 eV at the lattice constant of  $\text{MAPb}(\text{I}_2\text{Cl})$  while at its own lattice constant it is 1.49 eV as shown in table 2. Moreover, the energy gap varies in most cases less than 0.1 eV within the three possible cases concerning the position of the  $X'$  atom, with the maximum of 0.2 eV attended for the  $\text{MAPb}(\text{Cl}_2\text{I})$  and  $\text{MAPb}(\text{I}_2\text{Cl})$  compounds. Thus the exact arrangement of the X and  $X'$  halogen atoms is not crucial for the energy gap.

If we concentrate on the  $\text{MAGe}(\text{Pb})(\text{Cl}_2\text{I})$  and  $\text{MAGe}(\text{Pb})(\text{I}_2\text{Cl})$  compounds, the energy gaps of the mixed compounds are much closer to the values for the perfect  $\text{MAGe}(\text{Pb})\text{I}_3$  compound rather than those for the  $\text{MAGe}(\text{Pb})\text{Cl}_3$  compound, and the difference in the gap size with the latter can be as large as 1 eV, even in the case when we have two Cl and one I atoms. Thus, the change of the energy gap between the two parent compounds does not present a linear behavior, and the presence of iodine is predominant in determining the energy gap. When instead of I there is Br as in the  $\text{MAPb}(\text{Cl}_2\text{Br})$  and  $\text{MAPb}(\text{Br}_2\text{Cl})$  compounds, the behavior of the

Table 3

Calculated energy gaps in eV using the PBEsol functional for the mixed hybrid halide perovskites. We have assumed linear variation of the lattice constants between the extreme perfect compounds. Note that the terms ‘‘I, II and III’’ correspond to the position of the single halogen atom in the unit cell (see text for definitions). We have also calculated the energy gaps for the perfect compounds (last two lines in each case) at the lattice constants of the mixed hybrid halide perovskites.

	MAGe(Cl <sub>2</sub> I)	MAGe(I <sub>2</sub> Cl)		MACa(Cl <sub>2</sub> I)	MACa(I <sub>2</sub> Cl)
I-case	0.93	0.70	I-case	4.01	3.48
II-case	0.71	0.82	II-case	4.17	3.51
III-case	0.83	0.80	III-case	4.01	3.48
MAGeCl <sub>3</sub>	1.58	1.82	MACaCl <sub>3</sub>	4.75	4.25
MAGeI <sub>3</sub>	0.69	0.81	MACaI <sub>3</sub>	2.98	3.16
	MAPb(Cl <sub>2</sub> I)	MAPb(I <sub>2</sub> Cl)		MABa(Cl <sub>2</sub> I)	MABa(I <sub>2</sub> Cl)
I-case	1.41	1.51	I-case	4.04	3.66
II-case	1.52	1.40	II-case	4.00	3.65
III-case	1.61	1.30	III-case	4.04	3.62
MAPbCl <sub>3</sub>	2.44	2.52	MABaCl <sub>3</sub>	4.58	4.18
MAPbI <sub>3</sub>	1.01	1.30	MABaI <sub>3</sub>	3.34	3.26
	MAPb(Cl <sub>2</sub> Br)	MAPb(Br <sub>2</sub> Cl)		MABa(Cl <sub>2</sub> Br)	MABa(Br <sub>2</sub> Cl)
I-case	2.04	1.83	I-case	4.64	4.27
II-case	1.84	1.93	II-case	4.54	4.30
III-case	1.94	1.83	III-case	4.55	4.30
MAPbCl <sub>3</sub>	2.25	2.44	MABaCl <sub>3</sub>	4.69	4.67
MAPbBr <sub>3</sub>	1.53	1.73	MABaBr <sub>3</sub>	4.36	4.25

MAPb(X<sub>2</sub>X') energy gap changes and it is much closer to the perfect compound, with the three X atoms approaching a linear behavior. When instead of Ge(Pb) there is an alkali earth atom like Ca or Ba, the energy gap shows an almost linear behavior with the concentration of the halogen atoms between the two extreme parent compounds, even in the case where iodine is part of the halogen atoms contrary to the behavior of the MAGe(Pb)(Cl<sub>2</sub>I) and MAGe(Pb)(I<sub>2</sub>Cl) compounds.

Consequently, taking into account the fact that the energy gap of the perfect compounds depends strongly on the lattice constant, there is no simplified way to tune the properties of the mixed hybrid halid perovskites, the property is materials specific and should be determined in each case using electronic structure calculations.

## 6. Summary and conclusions

Perovskites are currently under intense investigation due to their potential applications in several devices ranging from solar cells to LEDs. Hybrid halide perovskites are of special interest combining the presence of an organic cation like methylammonium (MA), having the chemical formula CH<sub>3</sub>NH<sub>3</sub>, with the presence of halogen atoms. Especially MAPbI<sub>3</sub> has shown excellent properties regarding its usage in solar cell applications. However, the presence of lead prohibits it from a wide-spread use in industrial applications.

In an attempt to identify new hybrid halide perovskites which could substitute MAPbI<sub>3</sub>, we have studied using *ab-initio* electronic structure calculations the properties of MABX<sub>3</sub> compounds with the divalent cation B being one of the Ca, Sr, Ba, Zn, Cd, Hg, Ge, Sn or Pb atoms and considered all possible halogen atoms X= F, Cl, Br and I. The first step in our study was to use the VASP *ab-initio* technique



in conjunction with the so-called PBEsol functional for the exchange-correlation to determine the equilibrium lattice constants for all 36 compounds allowing the MA cation to relax within the cubic unit cell. We then proceeded to employ the more sophisticated hybrid HSE06 and mBJ+PBEsol functionals to calculate the electronic properties at the equilibrium and to estimate the band gap. We have shown that both lattice constants and energy gaps vary greatly depending on the choice for the divalent cation and the halogen atom. Compounds based on alkali earth atoms show very large band gaps, being transparent to light in the optical regime, while the compounds based on Zn, Cd and Hg show much smaller band gaps and some of them are even gapless semiconductors. Among them, MAZnCl<sub>3</sub> and MACdBr<sub>3</sub> are potential candidates to replace MAPbI<sub>3</sub>. Due to deterioration of the properties of the Sn-based compounds due to oxidation, the Ge compounds seem to be very promising and, more especially, our calculations suggest that MAGECl<sub>3</sub> and MAGEBr<sub>3</sub> are suitable to replace MAPbI<sub>3</sub> in devices. The width of the energy gaps depends on the kind of hybridization forming the gap. We have also performed calculations for the mixed hybrid halide perovskites mixing two kind of halogen atoms. Although we could tune the values for the energy band gaps, there is no simple pattern to predict the exact value based on the properties of the parent perfect compounds.

Consequently, we conclude that it is possible to find lead-free perovskites that can be used in energy technology applications like solar cells and optoelectronics, though the properties are materials specific and extended state-of-the-art, heavy *ab-initio* calculations are a prerequisite for any reliable result. We expect our results to intrigue further experimental studies on these compounds since, even if some of the calculated systems are ideal for a specific application, their growth and incorporation in devices still requires advanced synthesis techniques, which provide a difficult but promising challenge for the materials synthesis laboratories.

## Acknowledgements

Authors acknowledge financial support from the project PERMASOL (FFG project number: 848929).

## References

- [1] L. Yang, A.T. Barrows, D.G. Lidzey, T. Wang, Recent processes and challenges of organometal halide perovskite solar cells, *Rep. Prog. Phys.* 79 (2016) 026501.
- [2] M.A. Green, Silicon solar cells: evolution, high-efficiency design and efficiency enhancements, *Semiconduct. Sci. Technol.* 8 (1993) 1-12.
- [3] M.A. Pena, J.L.G. Fierro, Chemical structure and performance of perovskite oxides, *Chem. Rev.* 101 (2001) 1981-2017.
- [4] Q. Chen, N. De Marco, Y. Yang, T. Song, C. Chen, H. Zhao, Z. Hong, H. Zhou, Y. Yang, Under the spotlight: The organic-inorganic hybrid halide perovskite for optoelectronic applications, *Nano Today* 10 (2015) 355-396.
- [5] M. Grätzel, The light and shade of perovskite solar cells, *Nat. Mater.* 13 (2014) 838-842.
- [6] S.F. Hoeffler, G. Trimmel, T. Rath, Progress on lead-free metal halide perovskites for photovoltaic applications: a review, *Monatsh. Chem.* 148 (2017) 795.
- [7] G.C. Papavassiliou, G. Pagona, N. Karousis, G.A. Mousdis, I. Koutselas, A. Vassilakopoulou, Nanocrystalline/microcrystalline materials based on lead-halide units, *J. Mat. Chem.* 22 (2012) 8271-8280.
- [8] D. Weber, *Inst. Anorg. Chem. Univ. Stutt.* 33B (1978) 1443-1445.
- [9] M.B. Johnston, L.M. Herz, Hybrid Perovskites for Photovoltaics: Charge-Carrier Recombination, Diffusion, and Radiative Efficiencies, *Acc. Chem. Res.* (2015). DOI: 10.1021/acs.accounts.5b00411.
- [10] S. Brittman, G.W.P. Adhyaksa, E.C. Garnett, The expanding world of hybrid perovskites: materials properties and emerging applications, *MRS Commun.* 5 (2015) 7-26.
- [11] J. M. Frost, K.T. Butler, F. Brivio, C.H. Hendon, M. van Schilfgaarde, A. Walsh, Atomistic origins of high-performance in hybrid halide perovskite solar cells, *Nano Lett.* 14 (2014) 2584-2590.
- [12] A. Filippetti, A. Mattoni, Hybrid perovskites for photovoltaics: Insights from first principles, *Phys. Rev. B* 89 (2014) 125203.
- [13] J. Albero, A.M. Asiri, H. Garcia, Influence of the Composition of Hybrid Perovskites on their Performance in Solar Cells, *J. Mater. Chem. A* (2016). DOI: 10.1039/C6TA00334F.
- [14] Y. Zhou, M. Yang, O.S. Game, W. Wu, J. Kwun, M.A. Strauss, Y. Yan, J. Huang, K. Zhu, N.P. Padture, Manipulating Crystallization of Organolead Mixed-Halide Thin Films in Antisolvent Baths for Wide-Bandgap Perovskite Solar Cells, *ACS Appl. Mater. Interfaces* 8 (2016) 22322237.
- [15] Y. Zhao, K. Zhu, K. Organic-inorganic hybrid lead halide perovskites for optoelectronic and electronic applications, *Chem. Soc. Rev.* (2015). DOI: 10.1039/c4cs00458b.
- [16] C. Quarti, E. Mosconi, J.M. Ball, V. DInnocenzo, C. Tao, S. Pathak, H.J. Snaith, A. Petrozza, F. De Angelis, *Energy Environ. Sci.* 9 (2016) 155.
- [17] F. Brivio, A.B. Walker, A. Walsh, A. Structural and Electronic Properties of Hybrid Perovskites for

- High-Efficiency Thin-Film Photovoltaics from First-Principles, *APL Mater.* 1 (2013) 042111.
- [18] A. Walsh, Principles of chemical bonding and band gap engineering in hybrid organic-inorganic halide perovskites, *J. Phys. Chem. C* (2015). DOI: 10.1021/jp512420b.
- [19] A.M.A. Leguy, J.M. Frost, A.P. McMahon, V.G. Sakai, W. Kockelmann, C. Law, X. Li, F. Foglia, A. Walsh, B.C. O'Regan, J. Nelson, J.T. Cabral, P.R.F. Barnes, The dynamics of methylammonium ions in hybrid organic-inorganic perovskite solar cells, *Nature Commun.* 6 (2015) 7124.
- [20] F. Hao, C.C. Stoumpos, D.H. Cao, R.P.H. Chang, M.G. Kanatzidis, Lead-free solid-state organic-inorganic halide perovskite solar cells, *Nature Photonics* 8 (2014) 489-494.
- [21] C. Bernal, K. Yang, First-principles hybrid functional study of the organic-inorganic perovskites  $\text{CH}_3\text{NH}_3\text{SnBr}_3$  and  $\text{CH}_3\text{NH}_3\text{SnI}_3$ , *J. Phys. Chem. C* 118 (2014) 2438324388.
- [22] I. Borriello, G. Cantele, D. Ninno, Ab initio investigation of hybrid organic-inorganic perovskites based on tin halides, *Phys. Rev. B* 77 (2008) 235214.
- [23] T.J. Jacobsson, M. Pazoki, A. Hagfeldt, T. Edvinsson, Goldschmidt's rules and strontium replacement in lead halogen perovskite solar cells: Theory and preliminary experiments on  $\text{CH}_3\text{NH}_3\text{SrI}_3$ , *J. Phys. Chem. C* 119 (2015) 25673-25683.
- [24] E. Mosconi, A. Amat, M.L. Nazeeruddin, M. Grätzel, F.; De Angelis, First-principles modeling of mixed halide organometal perovskites for photovoltaic applications, *J. Phys. Chem. C* 117 (2013) 13902-13913.
- [25] C. Motta, F. El-Mellouhi, S. Sanvito, Charge carrier mobility in hybrid halide perovskites, *Nat. Sci. Reports* 5 (2015) 12746.
- [26] G. Kresse, J. Furthmüller, Efficient iterative schemes for *ab initio* total-energy calculations using a plane-wave basis set, *Phys. Rev. B* 54 (1996) 11169.
- [27] J. Kresse, D. Joubert, From ultrasoft pseudopotentials to the projector augmented-wave method, *Phys. Rev. B* 59 (1999) 1758.
- [28] J.P. Perdew, K. Burke, M. Ernzerhof, Generalized Gradient Approximation Made Simple, *Phys. Rev. Lett.* 77 (1998) 3865.
- [29] J.P. Perdew, A. Ruzsinszky, G.I. Csonka, O.A. Vydrov, G.E. Scuseria, L.A. Constantin, X. Zhou, K. Burke, K. Restoring the Density-Gradient Expansion for Exchange in Solids and Surfaces, *Phys. Rev. Lett.* 100 (2008) 136406; *ibid.* 102 (2009) 039902(E).
- [30] J. Heyd, G.E. Scuseria, M. Ernzerhof, M. Hybrid functionals based on a screened Coulomb potential, *J. Chem. Phys.* 118 (2003) 8207; *ibid.* 124 (2006) 219906(E).
- [31] J. Paier, M. Marsman, K. Hummer, G. Kresse, I.C. Gerber, J.G. Angyán, Screened hybrid density functionals applied to solids, *J. Chem. Phys.* 124 (2006) 154709; *ibid.* 125 (2006) 249901E.
- [32] A.D. Becke, E.R. Johnson, A simple effective potential for exchange, *J. Chem. Phys.* 124 (2006) 221101.
- [33] F. Tran, P. Blaha, Accurate Band Gaps of Semiconductors and Insulators with a Semilocal Exchange-Correlation Potential, *Phys. Rev. Lett.* 102 (2009) 226401.
- [34] [https://cms.mpi.univie.ac.at/vasp/vasp/meta\\_GGAs.html](https://cms.mpi.univie.ac.at/vasp/vasp/meta_GGAs.html)
- [35] C. Franchini, Hybrid functionals applied to perovskites, *J. Phys.: Condens. Matter*, 26 (2016) 253202.
- [36] H.J. Monkhorst, J.D. Pack, Special points for Brillouin-zone integrations, *Phys. Rev. B* 13 (1976) 135188.
- [37] T. Baikie, Y. Fang, J.M. Kadro, M. Schreyer, F. Wei, S.G. Mhaisalkar, M. Grätzel, T.J. White, Synthesis and crystal chemistry of the hybrid perovskite  $(\text{CH}_3\text{NH}_3)\text{PbI}_3$  for solid-state sensitised solar cell applications, *J. Mater. Chem. A* 1 (2013) 5628-5641.
- [38] Z. Pei, M. Friák, S. Sandlöbes, R. Nazarov, B. Svendsen, D. Raabe, J. Neugebauer, Rapid theory-guided prototyping of ductile Mg alloys: from binary to multi-component materials, *New H. Phys.* 17 (2015) 093009.